say for delineating deletion breakpoints, as exemplified in the analyses of Patients 1 and 4. Using a similar approach, we identified exonic deletions of *CHD7* in patients with CHARGE syndrome (Aramaki *et al.* 2006).

From a practical standpoint, it is important to note that the MP/LC assay developed here is also capable of identifying patients with whole *CREBBP* gene deletions, the frequency of which is reported to be approximately 10% among RTS patients (Petrij *et al.* 2000). Furthermore, the MP/LC assay uses the same equipment as the DHPLC system, which allows sensitive and specific screening of point mutations, small deletions, or small insertions (Udaka *et al.* 2005). Therefore, combining the MP/LC assay with DHPLC creates a comprehensive screening system for point mutations, small deletions/insertions, and large deletions of the *CREBBP* gene, all on the same platform.

In the present study, 45% of the patients did not have aberrations such as point mutations, small insertions or deletions, or exonic deletions in the *CREBBP* gene. Some of the RTS patients without detectable *CREBBP* mutations may have had mutations in the *EP300* gene, which was recently identified as a rare causative gene for RTS (Roelfsema *et al.* 2005). According to a *Drosophila* mutant screen study, numerous proteins interact with the *Drosophila* homolog of *CREBBP*. Thus, mutations in the human homologs of these *CREBBP*-interacting genes may also lead to a RTS-like phenotype. The patients who were negative for point mutations, small insertions/deletions, or exonic deletions in *CREBBP* should be further screened for mutations in *CREBBP*-interacting candidate genes.

ACKNOWLEDGMENT

REFERENCES

Aramaki M, Udaka T, Kosaki R, Makita Y, Okamoto N, Yoshihashi H, Oki H, Nanao K, Moriyama N, Oku S, Hasegawa T, Takahashi T, Fukushima Y, Kawame H, Kosaki K (2006) Phenotypic spectrum of CHARGE syndrome with *CHD7* mutations. J Pediatr 148:410–414.

Armour JA, Barton DE, Cockburn DJ, Taylor GR (2002) The detection of large deletions or duplications in genomic DNA. Hum Mutat 20:325–337.

Bartsch O, Schmidt S, Richter M, Morlot S, Seemanova E, Wiebe G, Rasi S (2005) DNA sequencing of *CREBBP* demonstrates mutations in 56% of patients with Rubinstein–Taybi syndrome (RSTS) and in another patient with incomplete RSTS. Hum Genet 117:485–493.

Blough RI, Petrij F, Dauwerse JG, Milatovich-Cherry A, Weiss L, Saal HM, Rubinstein JH (2000) Variation in microdeletions of the cyclic AMP-responsive element-binding protein gene at chromosome band 16p13.3 in the Rubinstein–Taybi syndrome. Am J Med Genet 90:29–34.

Breuning MH, Dauwerse HG, Fugazza G, Saris JJ, Spruit L, Wijnen H, Tommerup N, van der Hagen CB, Imaizumi K, Kuroki Y, van den Boogaard MJ, de Pater JM, Mariman ECM, Hamel BCJ, Himmelbauer H, Frischauf AM, Stallings RL, Beverstock GC, van Ommen GJB, Hennekam RCM (1993) Rubinstein–Taybi syndrome caused by submicroscopic deletions within 16p13.3. Am J Hum Genet 52:249–254.

Dehainault C, Lauge A, Caux-Moncoutier V, Pages-Berhouet S, Doz F, Desjardins L, Couturier J, Gauthier-Villars M, Stoppa-Lyonnet D, Houdayer C (2004) Multiplex PCR/liquid chromatography assay for detection of gene rearrangements: Application to *RB1* gene. Nucleic Acids Res 32:e139.

Kosaki K, Udaka T, Okuyama T (2005) DHPLC in clinical molecular diagnostic services. Mol Genet Metab 86:117–123.

Masuno M, Imaizumi K, Kurosawa K, Makita Y, Petrij F, Dauwerse HG, Breuning MH, Kuroki Y (1994) Submicroscopic deletion of chromosome region 16p13.3 in a Japanese patient with Rubinstein–Taybi syndrome. Am J Med Genet 53:352–354.

O'Donovan MC, Oefner PJ, Roberts SC, Austin J, Hoogendoorn B, Guy C, Speight G, Upadhyaya M, Sommer SS, McGuffin P (1998) Blind analysis of denaturing high-performance liquid chromatography as a tool for mutation detection. Genomics 52:44–49.

Petrij F, Giles RH, Dauwerse HG, Saris JJ, Hennekam RC, Masuno M, Tommerup N, van Ommen GJ, Goodman RH, Peters DJ, Breuning MH (1995) Rubinstein–Taybi syndrome caused by mutations in the transcriptional co-activator *CBP*. Nature 376:348–351.

Petrij F, Dauwerse HG, Blough RI, Giles RH, van der Smagt JJ, Wallerstein R, Maaswinkel-Mooy PD, van Karnebeek CD, van Ommen GJ, van Haeringen A, Rubinstein JH, Saal HM, Hennekam RC, Peters DJ, Breuning MH (2000) Diagnostic analysis of the Rubinstein–Taybi syndrome: Five cosmids should be used for microdeletion detection and low number of protein truncating mutations. J Med Genet 37:168–176.

Roelfsema JH, White SJ, Ariyurek Y, Bartholdi D, Niedrist D, Papadia F, Bacino CA, den Dunnen JT, van Ommen GJ, Breuning MH, Hennekam RC, Peters DJ (2005) Genetic heterogeneity in Rubinstein–Taybi syndrome: Mutations in both the *CBP* and *EP300* genes cause disease. Am J Hum Genet 76:572–580.

Roth DB, Wilson JH (1986) Nonhomologous recombination in mammalian cells: Role for short sequence homologies in the joining reaction. Mol Cell Biol 6:4295–4304.

Rubinstein J, Taybi H (1963) Broad thumbs and toes and facial abnormalities. Am J Dis Child 105:588–608.

Shaw CJ, Lupski JR (2004) Implications of human genome architecture for rearrangement-based disorders: The genomic basis of disease. Hum Mol Genet 13 Spec No 1:R57–R64.

Udaka T, Samejima H, Kosaki R, Kurosawa K, Okamoto N, Mizuno S, Makita Y, Numabe H, Toral JF, Takahashi T, Kosaki K (2005) Comprehensive screening of *CREB-binding protein* gene mutations among patients with Rubinstein–Taybi syndrome using denaturing high-performance liquid chromatography. Congenit Anom (Kyoto) 45:125–131.

Address reprint requests to:
Dr. Kenjiro Kosaki
Department of Pediatrics
Keio University School of Medicine
35 Shinanomachi, Shinjuku-ku
Tokyo 160-8582, Japan

E-mail: kkosaki@sc.itc.keio.ac.jp

Screening for CHARGE Syndrome Mutations in the *CHD7* Gene Using Denaturing High-Performance Liquid Chromatography

MICHIHIKO ARAMAKI,[1,3] TORU UDAKA,[1,3] CHIHARU TORII,[1] HAZUKI SAMEJIMA,[1] RIKA KOSAKI,[2] TAKAO TAKAHASHI,[1] and KENJIRO KOSAKI[1]

ABSTRACT

Mutations in the *CHD7* (*chromodomain helicase DNA binding protein 7*) gene cause CHARGE syndrome. At present, however, genetic testing of the *CHD7* gene is not commonly applied in clinical settings because the currently available assays are technically and financially demanding, mainly because of the size of the gene. In the present study, we optimized the highly sensitive and specific mutation scanning method automated denaturing high-performance liquid chromatography (DHPLC) to analyze the entire coding region of *CHD7*. The coding region was amplified by 39 primer pairs, all of which have the same cycling conditions, aliquoted on a 96-well format polymerase chain reaction (PCR) plate. In this manner, all of the exons were amplified simultaneously using a single block in a thermal cycler. We then wrote a computer script to analyze each segment of the *CHD7* gene by DHPLC in a serial manner using conditions that were optimized for each amplicon. The implementation of this screening method for *CHD7* will help medical geneticists confirm their clinical impressions and provide accurate genetic counseling to the patients with CHARGE syndrome and their families.

INTRODUCTION

CHARGE SYNDROME (MIM 214800) represents a constellation of nonrandomly associated malformations: C, coloboma of the iris or retina; H, heart defects; A, atresia of the choanae; R, retardation of growth and/or development; G, genital anomalies; and E, ear abnormalities. Mutations in the *chromodomain helicase DNA-binding protein 7* gene (*CHD7*) on chromosome 8q12.1 were identified as causative of this syndrome in 2004 (Vissers *et al.* 2004). Since then, two mutation analyses have been published regarding this locus (Jongmans *et al.* 2006; Sanlaville *et al.* 2006). At present, however, genetic testing of *CHD7* is not commonly applied in clinical settings because the currently available assays are technically and financially demanding, mainly because of the size of the *CHD7* gene, which comprises a coding sequence of 5,901 bp (Vissers *et al.* 2004).

Generally speaking, two approaches can be taken when performing genetic testing in clinical settings. Most intuitively, all of the coding exons can be amplified by PCR and then sequenced in parallel. This approach was used by Jongmans *et al.* (2006) and Sanlaville *et al.* (2006) in their mutational analyses of *CHD7*. Alternatively, screening procedures can be performed prior to the sequencing analysis to identify exon(s) that may harbor mutations. When the size of the gene (*i.e.*, the number of exons) is small, the first approach is more efficient. However, as the size of the gene increases, the second approach becomes more efficient from the standpoints of supply costs and labor.

Because the human *CHD7* gene is relatively large, consisting of 38 exons (Vissers *et al.* 2004), clinical genetic testing of *CHD7* is best accomplished by the second method. In the present study, we took advantage of a highly sensitive and specific automated denaturing high-performance liquid chromatography (DHPLC) technique (O'Donovan *et al.* 1998; Wagner *et al.*

[1]Department of Pediatrics, Keio University School of Medicine, Tokyo, Japan.
[2]Department of Clinical Genetics and Molecular Medicine, National Children's Medical Center,
[3]These authors equally contributed to this work.

1999; Udaka *et al.* 2005) to detect exon(s) that may harbor mutations prior to sequencing.

Mutation analysis by DHPLC involves subjecting PCR products to ion-pair reversed-phase liquid chromatography in a column containing alkylated nonporous particles. At the proper temperature, the heteroduplexes that form in PCR samples with internal sequence variations have a lower column retention time relative to their homoduplex counterparts. For analysis of autosomal recessive and X-linked recessive disorders, genomic DNA from normal individuals is added to each well so that a heteroduplex is formed if the patients are homozygous or hemizygous for the mutant allele. The major advantages of this method include rapid analysis (<5 min per PCR amplicon) and automated instrumentation. The greatest disadvantage of DHPLC is probably the high cost of the instrument. However, the user-friendliness of the software easily allows the development of programming that facilitates semiautomated operation. When semiautomated analysis of multiple exons (Kosaki *et al.* 2005) can be accomplished, as exemplified in this article, the system requires minimal human intervention, with a consequent significant reduction of the labor cost. This article presents in detail the methods we have developed for finding mutations in the *CHD7* gene that cause the majority of cases of CHARGE syndrome. Many of the mutations we have discovered using this methodology have been published previously together with a clinical description of the patients phenotype (Aramaki *et al.* 2006).

MATERIALS AND METHODS

Patients and DNA preparation

Thirty eight Japanese patients who fulfilled Blake's criteria for the diagnosis of CHARGE syndrome (Blake *et al.* 1998) were included in the study. The phenotypic spectrum of 24 of the 38 patients has been reported elsewhere (Aramaki *et al.* 2006). All of the patients were unrelated and simplex (*i.e.*, a single occurrence in a family). Each patient and their family members were enrolled in the study after receiving their written informed consent, according to a protocol approved by an institutional review board. Genomic DNA was isolated using the QIAamp system (Qiagen Inc. Valencia, CA).

PCR amplification of the genomic DNA

The entire *CHD7* coding region (exons 2–38; GenBank sequence accession number NM_017780) was screened for mutations. We carefully selected the primer pairs to insure that all of the primers could use the same cycling conditions. The primer pairs were designed to amplify the exons, exon–intron boundaries, and at least 20 base pairs (bp) of the flanking intron sequences. The optimized primer sequences are listed in Table 1. PCR was performed in a volume of 20 μl containing 30 ng of genomic DNA, 10 pmol each of the forward and reverse primers, 0.2 mM of each dNTP, 2 mM MgSO$_4$, 0.5 units of Platinum *Taq* DNA polymerase High Fidelity (Invitrogen, Tokyo, Japan), and the buffer supplied by the manufacturer. Thermal cycling was done using a touchdown PCR protocol (Don *et al.* 1991); the annealing temperature was decreased by 0.5°C every second cycle beginning at 63°C and decreasing to

a 'touchdown' annealing temperature of 58°C, which was then used for 30 cycles.

Mutation analysis

PCR amplicons from human genomic DNA were analyzed by DHPLC according to the method developed by Oefner and Underhill (O'Donovan *et al.* 1998; Wagner *et al.* 1999; Udaka *et al.* 2005) using an analysis system purchased from Transgenomic (Omaha, NE). To generate heteroduplexes, the PCR products were denatured at 95°C for 5 min and reannealed by cooling to 25°C with a temperature change of −1.5°C/min. After heteroduplex formation, the PCR amplicons were applied to a preheated reversed-phase column. An elution gradient was generated by mixing buffer A (0.1 M triethylammonium acetate) and buffer B (0.1 M triethylammonium acetate containing 25% [vol/vol] acetonitrile) in a linear gradient from start to a final %B over a period of 4.5 min, as described in Table 1. Standard operating procedures for the instrument's operation and maintenance and for mutation detection by DHPLC (http://cmgs.org/bpg/Guidelines/2002/dhplc.htm) have been described (Schollen *et al.* 2005).

All DHPLC conditions, including the melting temperatures and buffer gradients specific to each PCR amplicon, were determined using melting temperature prediction software (Transgenomic WAVEMAKER). Multiple column temperatures were used when the software predicted that the fragment being analyzed consisted of two or three different melting temperature domains. In that case, two or three analysis temperatures were needed to scan the entire exon sequence. Two or three temperature conditions were used for each amplicon, except for exons 3, 6, 7, 25, 30, 32, and 36, which were subjected to only a single condition. The optimized DHPLC conditions for each amplicon are listed in Table 1.

When the chromatographic analyses of all the amplicons were completed, the DHPLC profiles were visually compared with the profiles of normal controls. PCR products corresponding to all variant elution profiles of the DHPLC were purified using a desalting column and were sequenced bidirectionally using the dideoxy sequencing method (BigDye Dideoxy sequencing kit; Applied BioSystems, Foster City, CA) and an automated sequencer (ABI3100; Applied Biosystems). The sequence-verification primers were the same as the PCR primers.

RESULTS

Optimization of the PCR conditions

The coding region was amplified in 39 amplicons. The optimized sets of PCR primers are shown in Table 1. The 39 primer pairs, all with the same cycling conditions, were aliquoted on a 96-well format PCR plate. In this manner, all the exons were amplified simultaneously using a single block of a thermal cycler. The PCR plate will be referred to as the Condition-Oriented-PCR primer-Embedded-Reactor plate (COPPER plate) (Kosaki *et al.* 2005). All the exons were successfully amplified under a single condition without producing any artifacts from mispriming or primer–dimer formation (Fig. 1).

TABLE 1. PCR PRIMER SEQUENCES AND DHPLC ANALYSIS CONDITIONS
(TEMPERATURE AND GRADIENT) FOR CHD7 MUTATION SCREENING

Exon[a]	Forward/reverse[b]	Primer sequence (5'–3')	DHPLC temp (□)	DHPLC Gradient[c] (%B/4.5 min)
2a	F	gtttggaggagccgtgtgt	57.5	59–68
	R	atctgctgcatgtgctgagg	62.8	54–63
			65.8	51–60
2b	F	accagatacgagcccctac	59.6	59–68
	R	gactgtctggctccgagaac	62.1	57–66
			65.9	53–62
2c	F	cagattctccccgaatcctc	56.7	58–67
	R	ggatggggcatatttggata	58.0	57–66
			59.6	56–65
2d	R	ctcctcctccacaagtcagg	60.2	58–67
	R	catgttgaatttcacactgcaa	61.2	57–66
			62.2	56–65
3	F	catcagccactaactttcagttc	57.8	59–68
	R	tctcaatgttttgcagttgtttt		
4	F	aaagtgaacactaagcgatcca	57.5	51–60
	R	ataaccaaggctcgggaatc	58.7	48–57
5	F	ctcggccacattttctttt	57.7	54–63
	R	gctgaaagtccaatgcttcc	60.3	51–60
6	F	gtggtagcaaaggggaatga	58.1	50–59
	R	caaagccaacaatcctgtaaga		
7	F	gtgaaggtcctttgctgctc	54.9	56–63
	R	ccaggccatgatgactaaa		
8	F	tgttgctcagcagccttaat	55.4	54–63
	R	atgcaagttgacagcaccaa	56.5	52–61
9	F	aactttttttttccctttggtg	57.4	51–60
	R	tccaaggctctgaccaagac	59.6	48–57
10 & 11	F	tgtatgtggtcaaatgaatccaa	54.0	59–68
	R	ttcaataactaaaggaaaggaactaca	56.8	57–66
			59.2	54–63
12	F	agcctttgggtatgcatttg	56.0	57–66
	R	ccttcccaagtcaccaagac	58.6	54–63
13	F	gagatctccaaagggataaatacg	56.2	53–62
	R	gcatcaaattctgagcaacg	59.4	50–59
14	F	ggtgtctagtgagaggctctgg	56.8	54–63
	R	tgccatttcatgggctaatc	60.1	48–57
15	F	cactgggctttgaaaaatgaa	56.3	57–66
	R	caccatgaaatccccagtct	58.2	55–64
16	F	cagtttgcaatgggttttga	58.1	53–62
	R	gacccctgggaaggtaattt	60.5	51–60
17	F	ctatgcgtcaggcctcctt	59.0	53–62
	R	tgggtctgactggtactctctgt	60.8	50–59
18	F	tttggtggggagacagaaac	56.7	54–63
	R	tgaggtcgaaaaataatcaaagg	57.7	52–61
19	F	tgcagcatttgtttagtctgc	55.8	56–65
	R	ttcccaatgcatcttgtaagc	58.0	54–63

Exon[a]	Forward/reverse[b]	Primer sequence (5'–3')	DHPLC temp (□)	DHPLC Gradient[c] (%B/4.5 min)
20 & 21	F	gaaaggcctctcaaagtaatgc	56.4	59–68
	R	ggggtgtcacacaaattcaa	58.0	57–66
			59.5	54–63
22	F	cacccagtgtgaattgttgc	59.3	56–65
	R	aagttcctggtggctttgtg	60.5	54–63
23	F	gcctcgtgcattaagctctc	58.0	55–64
	R	cctccaaatctgcgagttct	59.8	53–62
			63.0	49–58
24	F	atgatggatgaacagcagca	60.6	52–61
	R	gttttccggctacccagatt	61.4	50–59
25	F	cccaccatgctcagatgttt	57.8	53–62
	R	tggtagacgccaagagtcct		
26	F	gttgtggcagtgctgtgatt	59.6	54–63
	R	gaaccctgccaatagatgtga	62.7	51–60
27 & 28	F	ccccctтccттcттттgct	54.4	57–66
	R	ccacgtgaacaatgactgct	56.7	53–62
29	F	cccttтcccacactgtcatt	60.0	55–64
	R	gagccttctttggtggtca	61.5	53–62
30	F	ccacccccaaataactacca	57.9	54–63
	R	tttacttggggagaattcaagg		
31a	F	cccttgaattctccccaagt	58.7	58–67
	R	cttcggcttgttccagtacc	62.1	54–63
31b	F	actggcagttggatttgtcc	59.0	58–67
	R	cagaaagcaacgcatctcac	60.5	57–66
32	F	tttccctgatactgtggttgtg	59.3	51–60
	R	ccctaatcctтttggtcagc		
33	F	ctctтtтgcatcttgatggatg	57.1	57–66
	R	tttctaagcaaggccagtgaa	58.8	55–64
			60.8	53–62
34	F	ttggctcactgcaactctgt	57.9	58–67
	R	agctgtcaacacgtgcaatc	60.1	56–65
35	F	ttgtcagaggctctctcttcg	57.7	55–64
	R	cctgcaagattccttccaac	59.5	53–62
36	F	tctgacagttctctтtggcatt	57.3	50–59
	R	ccttctgggctaagaaatcg		
37	F	aacagaaaggggagggaaga	57.4	52–61
	R	ctgaataattaatggccaacagaa	59.7	46–55
38a	F	gttcaccacagaggctcaca	59.8	58–67
	R	gaagtgctgtcttccggttc	62.4	56–65
			63.4	55–64
38b	F	tgtcagctgctactggaaaca	55.5	61–70
	R	tttaaacacttgaactggaactgg	58.8	59–68
			61.5	56–65

[a]Some exons are amplified in multiple PCRs, designated a, b, etc., and some PCRs contain more than one exon.
[b]Forward, upstream primer; reverse, downstream primer.
[c]Buffer A is 0.1 M triethylammonium acetate; Buffer B is 0.1 M triethylammonium acetate containing 25% (vol/vol) acetonitrile. "54–63" indicates that the gradient consists of 54% B: 46% A through to 63% B: 37% A.
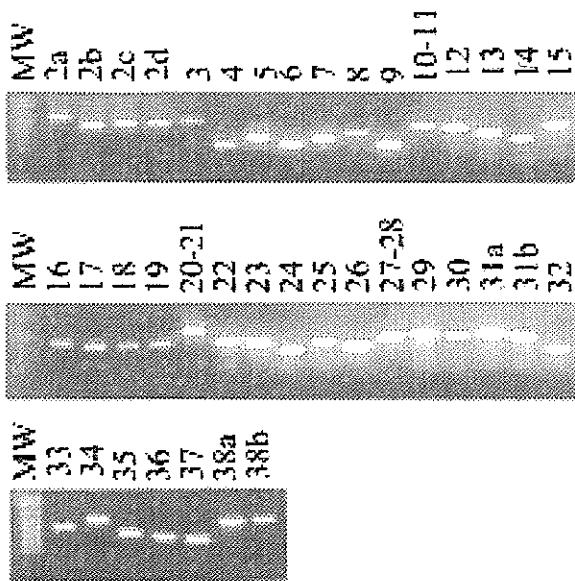
FIG. 1. PCR amplification for all coding exons of *CHD7* using the same amplification conditions. Here, 1% agarose gel electrophoresis of all 39 amplicons covering the entire coding region of *CHD7* is shown. The leftmost lane (MW) in each gel contains 1-kb ladder markers corresponding to 100-, 200-, 300-, 400-, 500-, 650-, 850-, and 1,000-bp fragments; the other lanes were loaded with 3 μl of PCR products. Please note that this figure was presented for illustrative purposes. We do not usually subject each plate to agarose gel electrophoresis prior to DHPLC analysis.

Optimization of the DHPLC conditions

The predicted optimal column temperatures and elution gradient for the DHPLC analysis of each PCR amplicon were verified by confirming that the elution profile of each of the PCR amplicons generated from wild-type genomic DNA (Kosaki *et al.* 2005; Udaka *et al.* 2005) had a sharp and solitary peak. The optimized column temperatures and elution gradients for the DHPLC analysis of each PCR amplicon are shown in Table 1. Figure 2 shows DHPLC profiles for the mutations discovered in our patient population, including several mutations that were reported previously (Aramaki *et al.* 2006).

Several specific factors are known to affect the sensitivity of the DHPLC assay. First, the use of impure oligonucleotide primers for PCR amplification can yield false-positive results (Kosaki *et al.* 2005). Second, poor quality of the DNA polymerase can also yield false-positive results (Kosaki *et al.* 2005). Third, the fragment size can affect the sensitivity of the assay; the optimal fragment size ranges from 150 bp to 700 bp (Xiao and Oefner 2001). Fourth, a high G-C content may affect the performance of the DHPLC (Escary *et al.* 2000). We have taken all of these factors into account in the design of the assay.

The DHPLC analysis system used in the present study (Transgenomic) allowed us to write a computer script to analyze all the PCR amplicons generated from various portions of the *CHD7* gene in a serial manner at optimized conditions determined individually for each amplicon. This script enabled

us to analyze the entire gene overnight in an automated manner. The complete script is available on our Web site at http://www.dhplc.jp, both in text and binary format. The binary format script can be directly loaded onto the controlling units of Transgenomic DHPLC systems.

Mutation analysis of patients with CHARGE syndrome

The mutations identified in the present study are summarized in Table 2. Including mutations previously reported (Aramaki *et al.* 2006), we identified heterozygous *CHD7* mutations in 26 (68%) of the 38 patients enrolled in the study, including 8 frameshift mutations, 12 nonsense mutations, 5 splice-site mutations, and 1 missense mutation. All identified mutations were private, except for a R1494X nonsense mutation of exon19 (4480C → T), which was detected in 2 unrelated patients, and a IVS25-7G → A splicing mutation previously reported by others (Vissers *et al.* 2004). Known single-nucleotide polymorphisms (SNPs) in the *CHD7* gene that are published in the dbSNP database (http://www.ncbi.nlm.nih.gov/projects/SNP/) were detected, including rs16926453, rs2272727, and rs3763592.

Nonsense mutations, as well as deletions and insertions leading to frameshifts, can unambiguously be identified as disease-causing mutations. The G → T mutations that occurred at the invariant G base of the splice-donor sites flanking exons 18 and 26 and the A → G mutations that occurred at the invariant A base of the splice-acceptor site flanking exon 22, are most likely pathogenic as well. Two intronic sequence variants present in the proximity of exon–intron boundaries (IVS25-7G → A and IVS30+5G → C) are also likely to be pathogenic in that these mutations occurred *de novo* and were not found in 100 ethnically matched controls. One heterozygous missense substitution, S699N, was identified in exon 3. This missense substitution is likely to be pathogenic in that this substitution occurred *de novo* and was not found in 100 ethnically matched controls. The S699 residue was conserved in the chimpanzee, but not in the rat.

We further attempted to quantify the pathogenicity of these sequence variants by using the NNSplice program (http://www.fruitfly.org/seq_tools/splice.html) (Reese *et al.* 1997). The NNSplice program calculates the probability of splicing at a specific splicing site. The IVS30+5G → C mutation reduces the probability score from 0.98 to 0.15. We were not able to assess the effect of IVS25-7G → A. Because the base substitution 2096G → A leading to S699N occurred at the 3′-most base within exon 3, the substitution might have affected the splicing. According to the NNSplice program, the 2096G → A mutation reduces the probability score from 0.96 to 0.40. These data support the notion that the IVS30+5G → C mutation and the 2096G → A mutation may affect normal splicing.

DISCUSSION

In the present study, we developed a DHPLC-based method allowing the entire coding region of the *CHD7* gene to be screened for point mutations and small deletions and insertions. Mutations were identified in more than two thirds (26 out of 38) of the patients who had been clinically diagnosed as hav-
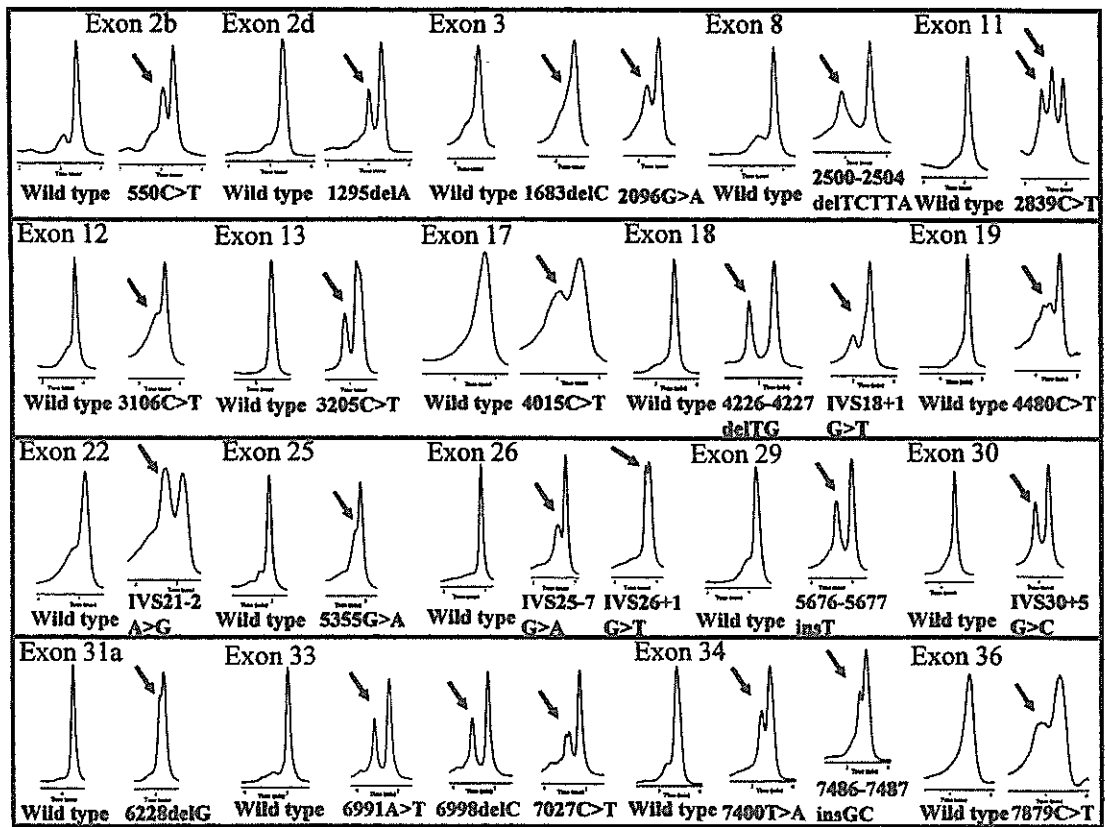
FIG. 2. DHPLC elution profiles of *CHD7* mutations detected in the present study and in our previous study (Aramaki *et al.* 2006). The column temperatures were 65.9°C, 60.2° C, 57.8°C, 55.4°C, 59.2°C, 58.6°C, 56.2°C, 60.8°C, 57.7°C, 58.0°C, 60.5°C, 57.8°C, 62.7°C, 60.0°C, 57.9°C, 62.1°C, 60.8°C, 57.9°C, and 57.3°C for exons 2b, 2d, 3, 8, 11, 12, 13, 17, 18, 19, 22, 25, 26, 29, 30, 31a, 33, 34, and 36, respectively. Only the chromatogram with the best resolution of the heteroduplex peak is shown for each mutation.

ing the CHARGE syndrome. No predominant mutations or mutation clusters were observed within the *CHD7* gene. The majority of the mutations were predicted to lead to a premature translation stop. The phenotypic spectrum of mutation-positive patients has already been discussed elsewhere (Aramaki *et al.* 2006) and will not be further discussed herein. Our mutation

detection rate of 68% (26/38) was comparable to that reported by Jongmans *et al.* (2006) (64%, 69/107), but lower than that reported by Sanlaville *et al.* (2006) (100%, 10/10). The difference in the mutation detection rate may have arisen from differences in the inclusion criteria, in that the present study and Jongmans *et al.* study dealt with postnatal cases, whereas that

TABLE 2. *CHD7* MUTATIONS IDENTIFIED IN THIS STUDY

Exon	Type	Mutation	Amino acid substitution	De novo
3	Missense	2096G → A	S699N	Yes
13	Nonsense	3205C → T	R1069X	ND
18	Frameshift	4226–4227delTG	V1409EfsX1420	Yes
22	Splice site	IVS21-2A → G	NA	ND
25	Nonsense	5355G → A	W1785X	ND
30	Splice site	IVS30+5G → C	NA	Yes
33	Nonsense	7027C → T	Q2343X	ND
34	Nonsense	7400T → A	L2467X	ND
36	Nonsense	7879C → T	R2627X	ND

Abbreviations: ND, not determined; NA, not applicable.

by Salanville *et al.* used aborted fetuses. The follow-up study (Jongamans *et al.* 2006) of the postnatal cohort reported by Vissers *et al.* (2004) revealed a high rate of mutation detection (95%, 18/19). The difference in mutation detection between our study and Vissers *et al.* (2004) may be explained by differences in the patient ascertainment; we recruited patients from pediatric clinics, whereas Vissers *et al.* recruited patients from otolaryngology clinics.

In 12 of the 38 patients we did not find a micromutation using DHPLC. Several factors may be responsible for a detection rate of less than 100%. First, some patients may have large deletions spanning one or several exons or even the entire *CHD7* locus that would be undetectable using our methodology. Large deletions can be detected on a DHPLC platform using a recently developed method called multiplex PCR/liquid chromatography assay (Dehainault *et al.* 2004). A multiplex PCR with unlabeled primers enables simultaneous amplification of multiple exons under semiquantitative conditions and the PCR products separated by DHPLC are quantitated by fluorescence detection. Indeed, 1 patient in our cohort was found to have a deletion spanning several exons (Udaka *et al.* 2006). Second, these patients may have mutations deep within introns or in other parts of the *CHD7* gene that were not studied, such as the promoter. Third, there may be mutations in other genes, including *SEMA3E*, which has recently been identified as a rare causative gene for the CHARGE syndrome (Lalani *et al.* 2004). Fourth, some patients enrolled in the present study may have a different condition that resembles CHARGE syndrome. Alternatively, the sensitivity of our DHPLC assay may be less than 100%. Without performing comparative analysis of the same set of samples by direct sequencing, we were not able to determine the sensitivity of the DHPLC assay. However, previous work on another gene (*PTPN11*) indicates that the sensitivity figures for DHPLC and sequencing may be comparable (Kosaki *et al.* 2005).

The computer program installed in the DHPLC system does not automatically call mutations, *i.e.*, a human eye still needs to look over the traces and call the mutations. However, inspection of a chromatogram from 1 patient takes only a few seconds and thus the process does not represent a bottleneck in the mutation analysis process. The ease of inspection of a DHPLC chromatogram contrasts with the difficulty of inspection of a sequencing chromatogram. Indeed, the Dutch group (Vissers *et al.* 2004), which reported a detection rate of 68% (10/17) by direct sequencing in an initial study, later found that reanalysis of the same set of 17 patients by direct sequencing identified 6 additional patients with mutations (Jongmans *et al.* 2006). Hence, direct sequencing failed to detect a mutation in a significant proportion of patients (6/17) in the initial study. This observation illustrates the potential difficulty in mutation calls in direct sequencing.

The use of the COPPER plate (Kosaki *et al.* 2005) enables all of the exons to be simultaneously amplified on a 96-well format PCR plate under the same cycling conditions, whereas the use of the computer script enables a completely automated DHPLC analysis of all the exons. These two features minimize the labor required by laboratory workers. The implementation of the screening method for *CHD7* described herein will help medical geneticists confirm their clinical impressions and provide accurate genetic counseling to the patients and their families with CHARGE syndrome. Precise documentation of *CHD7* mutations has clinical ramifications in the genetic counseling of CHARGE syndrome patients, in that gonadal mosaicism has been documented in this syndrome (Jongmans *et al.* 2006). Lack of the mutant allele in the parents' peripheral blood or father's sperm will be informative for the parents in terms of a low recurrence risk. The possibility of prenatal diagnosis in subsequent pregnancies could further reassure the parents.

REFERENCES

Aramaki M, Udaka T, Kosaki R, Makita Y, Okamoto N, Yoshihashi H, Oki H, Nanao K, Moriyama N, Oku S, Hasegawa T, Takahashi T, Fukushima Y, Kawame H, Kosaki K (2006) Phenotypic spectrum of CHARGE syndrome with CHD7 mutations. J Pediatr 148: 410–414.

Blake KD, Davenport SL, Hall BD, Hefner MA, Pagon RA, Williams MS, Lin AE, Graham JM, Jr (1998) CHARGE association: an update and review for the primary pediatrician. Clin Pediatr (Phila) 37:159–173.

Dehainault C, Lauge A, Caux-Moncoutier V, Pages-Berhouet S, Doz F, Desjardins L, Couturier J, Gauthier-Villars M, Stoppa-Lyonnet D, Houdayer C (2004) Multiplex PCR/liquid chromatography assay for detection of gene rearrangements: application to RB1 gene. Nucleic Acids Res 32:e139.

Don RH, Cox PT, Wainwright BJ, Baker K, Mattick JS (1991) 'Touchdown' PCR to circumvent spurious priming during gene amplification. Nucleic Acids Res 19:4008.

Escary JL, Cecillon M, Maciazek J, Lathrop M, Tournier-Lasserve E, Joutel A (2000) Evaluation of DHPLC analysis in mutational scanning of Notch3, a gene with a high G-C content. Hum Mutat 16:518–526.

Jongmans MC, Admiraal RJ, van der Donk KP, Vissers LE, Baas AF, Kapusta L, van Hagen JM, Donnai D, de Ravel TJ, Veltman JA, Geurts van Kessel A, De Vries BB, Brunner HG, Hoefsloot LH, van Ravenswaaij CM (2006) CHARGE syndrome: the phenotypic spectrum of mutations in the CHD7 gene. J Med Genet 43:306–314.

Kosaki K, Udaka T, Okuyama T (2005) DHPLC in clinical molecular diagnostic services. Mol Genet Metab 86:117–123.

Lalani SR, Safiullah AM, Molinari LM, Fernbach SD, Martin DM, Belmont JW (2004) SEMA3E mutation in a patient with CHARGE syndrome. J Med Genet 41:e94.

O'Donovan MC, Oefner PJ, Roberts SC, Austin J, Hoogendoorn B, Guy C, Speight G, Upadhyaya M, Sommer SS, McGuffin P (1998) Blind analysis of denaturing high-performance liquid chromatography as a tool for mutation detection. Genomics 52:44–49.

Reese MG, Eeckman FH, Kulp D, Haussler D (1997) Improved splice site detection in Genie. J Comput Biol 4:311–323.

Sanlaville D, Etchevers HC, Gonzales M, Martinovic J, Clement-Ziza M, Delezoide AL, Aubry MC, Pelet A, Chemouny S, Cruaud C, Audollent S, Esculpavit C, Goudefroye G, Ozilou C, Fredouille C, Joye N, Morichon-Delvallez N, Dumez Y, Weissenbach J, Munnich A, Amiel J, Encha-Razavi F, Lyonnet S, Vekemans M, Attie-Bitach T (2006) Phenotypic spectrum of CHARGE syndrome in fetuses with CHD7 truncating mutations correlates with expression during human development. J Med Genet 43:211–317.

Schollen E, Dequeker E, McQuaid S, Vankeirsbilck B, Michils G, Harvey J, van den Akker E, van Schooten R, Clark Z, Schrooten S, Matthijs G, Group DC (2005) Diagnostic DHPLC Quality Assurance (DDQA): a collaborative approach to the generation of validated and standardized methods for DHPLC-based mutation screening in clinical genetics laboratories. Hum Mutat 25:583–592.

Udaka T, Torii C, Takahashi D, Mori T, Aramaki M, Kosaki R, Tani-gawara Y, Takahashi T, Kosaki K (2005) Comprehensive screening of the thiopurine methyltransferase polymorphisms by denaturing high-performance liquid chromatography. Genet Test 9:85–92.

Udaka T, Okamoto N, Aramaki M, Torii C, Kosaki R, Hosokai N, Hayakawa T, Takahata N, Takahashi T (2006) An Alu retrotransposition-mediated deletion of CHD7 in a patient with CHARGE syndrome. Am J Med Genet (in press).

Vissers LE, van Ravenswaaij CM, Admiraal R, Hurst JA, de Vries BB, Janssen IM, van der Vliet WA, Huys EH, de Jong PJ, Hamel BC, Schoenmakers EF, Brunner HG, Veltman JA, van Kessel AG (2004) Mutations in a new member of the chromodomain gene family cause CHARGE syndrome. Nature Genet 36:955–957.

Wagner T, Stoppa-Lyonnet D, Fleischmann E, Muhr D, Pages S, Sandberg T, Caux V, Moeslinger R, Langbauer G, Borg A, Oefner P (1999) Denaturing high-performance liquid chromatography detects reliably BRCA1 and BRCA2 mutations. Genomics 62:369–376.

Xiao W, Oefner PJ (2001) Denaturing high-performance liquid chromatography: A review. Hum Mutat 17:439–474.

AU3

Address reprint requests to:
Dr. Kenjiro Kosaki
Department of Pedaitrics
Keio University School of Medicine
35 Shinanomachi, Shinjuku-ku
Tokyo 160-8582, Japan

E-mail: kosaki@sc.itc.keio.ac.jp

原 著

4カラーデジタルフローサイトメーターを用いた
小児白血病マーカー中央診断の試み

塩沢裕介[1,2,3]，　北村紀子[1,2]，　竹野内寿美[1,2]，　田口智子[1,2]

大喜多肇[1]，　林　泰秀[4,5]，　小原　明[4,6]，　花田良二[4,7]

土田昌宏[4,8]，　藤本純一郎[1,4]，　清河信敬[1,2]

A trial of central diagnosis of childhood acute lymphoblastic leukemia
with 4-color digital flow cytometer

Yusuke Shiozawa M.D., Ph.D.[1,2,3], Noriko Kitamura Ph.D.[1,2], Hisami Takenouchi Ph.D.[1,2],
Tomoko Taguchi M.D., Ph.D.[1,2], Hajime Okita M.D., Ph.D.[1], Yasuhide Hayashi M.D., Ph.D.[4,5],
Akira Ohara M.D., Ph.D.[4,6], Ryoji Hanada M.D., Ph.D.[4,7], Masahiro Tuchida M.D., Ph.D.[4,8],
Junichiro Fujimoto M.D., Ph.D.[1,4], Nobutaka Kiyokawa M.D., Ph.D.[1,2]

[1] Department of Developmental Biology, National Research Institute for Child Health and Development
[2] Central Diagnosis Center, Tokyo Children's Cancer Study Group
[3] Department of Pediatrics, Juntendo University School of Medicine
[4] Tokyo Children's Cancer Study Group
[5] Gunma Children's Medical Center
[6] Department of Blood Transfusion, Toho University Omori Medical Center
[7] Department of Hematology and Oncology, Saitama Children's Medical Center
[8] Ibaraki Children's Hospital

Aim. We are in charge of the central diagnosis and cell preservation as a part of childhood acute lymphoblastic leukemia treatment study in Tokyo Children's Cancer Study Group. It is necessary to diagnose with a minimal quantity of specimen, to preserve leukemic cells effectively as possible. Therefore a diagnosis of childhood acute lymphoblastic leukemia by four-color analysis with digital flow cytometer has been examined.

Methods. We examined cell markers of childhood acute lymphoblastic leukemia cells by four-color analysis using digital flow cytometers. We selected the monoclonal antibodies for the diagnosis based on the recommendation of Japan Pediatric Lymphoma Study Group and made out a panel of antibodies which enable us to confirm aberrant antigen-expressions on the leukemic cells.

Results. Four colors that we used in this study were fluorescein isothyocyanate, phycoerythrin, phycoerythrin-cyanin 5.1, and phycoerythrin-cyanin 7. The most of childhood acute lymphoblastic leukemia cases could be diagnosed without CD45-gating. List mode compensation was useful to re-investigate specimens which was difficult to re-examine, because there were very few.

Discussion. Four-color analysis using digital flow cytometer is useful to save precious specimen of childhood acute lymphoblastic leukemia. We are intending to perform five-color analysis with CD45-gating as a next step.

[1] 国立成育医療センター研究所　発生・分化研究部
[2] TCCSG（東京小児がん研究グループ）　中央診断センター
[3] 順天堂大学医学部　小児科
[4] TCCSG（東京小児がん研究グループ）
[5] 群馬県立小児医療センター
[6] 東邦大学医学部大森病院　輸血部
[7] 埼玉県立小児医療センター　血液・腫瘍科
[8] 茨城県立こども病院

はじめに

2004年12月より開始された東京小児がん研究グループ（Tokyo Children's Cancer Study Group, TCCSG）の小児急性リンパ芽球性白血病(Acute Lymphoblastic Leukemia, ALL)に対する多施設共同治療研究第16次案（TCCSG ALL L04-16）では，診断の施設間格差を標準化する目的で白血病の細胞マーカーの中央診断を行っている。また，余剰検体を今後の白血病研究に有効活用することを目的に，インフォームド・コンセントを得た上での細胞保存も開始された。この中央診断と細胞保存のセンターとしての役割を，国立成育医療センター研究所　発生・分化研究部が担当している。なるべく多くの細胞を保存することを優先し，かつ中央診断として充分な項目を検査するためには，必要最小限の検体量で効率的に細胞マーカー診断を行う必要がある。

そこで，われわれは，デジタルフローサイトメーター（DG-FCM）を用いた4カラー解析での細胞マーカー解析の有用性について検討した。

方　　法

白血病細胞株，健常人および小児ALL症例の血液あるいは骨髄検体に対し，fluorescein isothyocyanate（FITC），phycoerythrin（PE），PE-cyanin 5.1（PC-5）またはallophycocyanin（APC），PC-7を用いた4カラー染色を行い，DG-FCM EPICS® XL™（BECKMAN COULTER, Miami, FL）および Cytomics™ FC500（BECKMAN COULTER）を用いて解析した。

モノクローナル抗体（monoclonal antibody, MoAb）のパネルはJapan Pediatric Lymphoma Study Group（JPLSG）"小児造血器腫瘍の免疫学的診断の標準化ワーキング・グループ"の推奨検査項目を基本に，その他有用と考えられる抗体を追加，選択した。蛍光補正を容易にするため，原則的に各組にB-lineage，T-lineage，Myeloid-lineage，と非-lineage，各1項目ずつを組み合わせ，小児で最も頻度が高いB-precursor ALLを想定して作成した（Table 1）。aberrantな抗原の発現が確認可能なMoAbの組み合わせを考慮し，minimal residual disease（MRD）検出も視野に入れた。一部の項目についてはクローンや標識の違いによる検出率の差について比較するため，複数の抗体を併用した。

Table 1

	FITC		PE						

Cell surface
細胞裏面

1	IgG1	BC IM0639							
2	kappa (Poly)		lamda (Poly)			CD19	DK TC051	CD45	BC IM3548
3	CD99	BD 555668							
4	CD65	BC IM1654	7.1	BC IM3454	HLA-DR	BC IM2657	CD34	BC A07509
5	CD66C	BC IM2038							
6	mue (Poly)	DK F0056	CD56	BC IM2073	CD10	BC IM2721	CD20	BC IM3629
7	gamma (Poly)	DK F0056							
8	CD49d	BC IM1404	CD18	BC IM1570	CD4	BC IM2636	CD8	BC 6607102
9	CD49e	BC IM1854							
10	CD44	BC IM1219	CD45RA	BC IM1834	TCR-g/d	BC IM2662	CD14	BC A22331
11	CD58	BC IM1218							
12	CD11b	BC IM0530	C42b	BC IM1447	CD244	BC IM2658	CD16	BC 6607118
13	CD184	DK RF170	Glycophorin A	BC 6607066				
14	CD62L	BC IM1231	CD27	BC IM2578	TCR a/b	BC IM2661	CD61	BC IM3716

Cytoplasmic
細胞質内(Pharmingen, Fix/Permを使用)

21	IgG1	BC IM0639	IgG1	BC IM731599					
22	TdT	DK F7139	MPO	BD 341642	CD79a	BC IM3456	CD3	BC 6607100
23	mue	BD 555782	CD179a(HSL96)						
24	Pre-BCR(HSL2)		CD22	DK R7061					

HSL2およびHSL96は、東京医科歯科大学院大学医歯学総合研究科・免疫アレルギー学分野　烏山一先生から分与いただいたものを精製、蛍光標識して用いている。
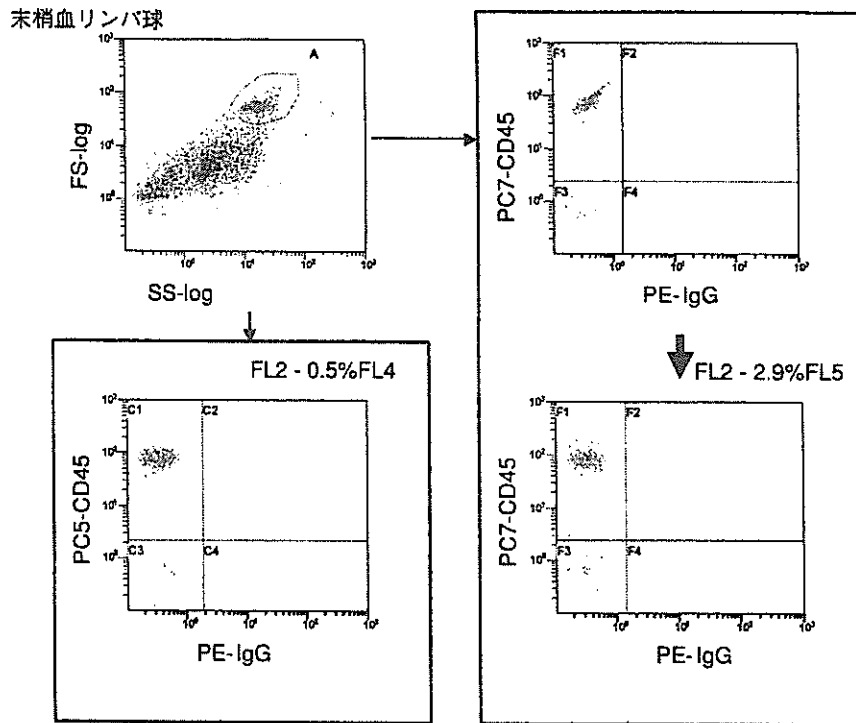BC, Beckman Coulter社、BD, Becton Dickinson社、DK, Dako社

Figure 1 タンデム色素のPEチャンネルへの漏れ込み
FC500を用いて，PEをドナーとするタンデム色素，PC5とPC7のPEチャンネルへの漏れ込みについて
検討した。いずれも，若干の補正が必要であった。

CD45-gatingに関しては，1）同じ検体量でなるべく多項目を検査するため，2）通常各施設の検査ではCD45-gatingを行っているのでこれと比較することが可能であること，等の理由により 基本的に用いなかった。

また，診療施設から中央診断への検体の送付，余剰検体の保存については，関係各施設の倫理委員会の承認後，L04-16に登録する際に本人あるいは保護者のインフォームド・コンセントを得た上で行っている。

結　　果
染色色素の選択

PEをドナーとするタンデム色素のPEチャンネルへの漏れ込みについて，比重遠心法により分離した健常人末梢血単核球をそれぞれの蛍光色素で標識した抗CD45抗体で染色して検討した。蛍光の他のチャンネルへの漏れ込みは，測定条件やPhoto multiplier tube（PMT）の性能に大きく依存すると考えられる。今回の検討では，XLで測定した場合，現在の使用条件においては，PC-5のPEへの漏れ込みはほとんど認められなかったが， PC-7のPEへの漏れ込みは補正が必要で

あった。FC500で測定した場合には，PC-5のPEへの漏れ込みについても若干補正が必要であった（Figure 1）。phycoerythrin-Texas Red（ECD）は，PE以外にも，他のチャンネルへの漏れ込みが強く，抗体の組み合わせによっては，蛍光補正が難しい場合があった。

PC-5とAPCの比較を行った。CD3およびCD19について，同一クローンの抗体をそれぞれの色素で標識したもので同一の健常人末梢血単核球検体を染色し，FC500を用いて蛍光強度の比較を行ったが，PC-5とAPCでほぼ同等の蛍光強度が得られた。以上の結果に基づいて，シングルレーザーで行える簡便性からPC-5を標準的に採用し，これにFITC，PE，PC-7を加えた4色を選択した。

症例の解析

標準的な2カラー染色，あるいはCD45-gatingを加えた3カラー染色による解析ですでに診断のついている小児白血病検体を用いて，4カラー染色による染色性を比較検討した。同じ抗原に対する抗体であっても，用いるクローンによっては反応性が大きく異なる場合も想定される。しかし，同一クローンを用いた場合で
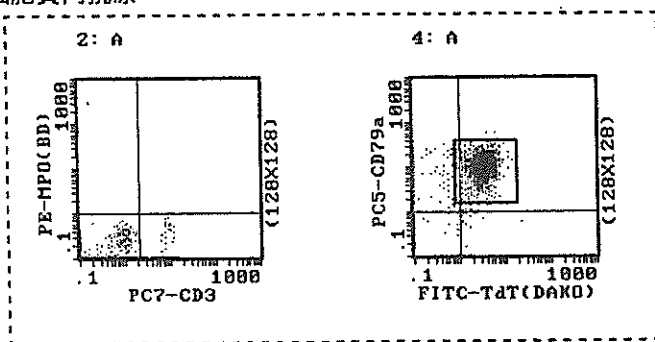
症例1（FS/SS-gating）

細胞表面抗原
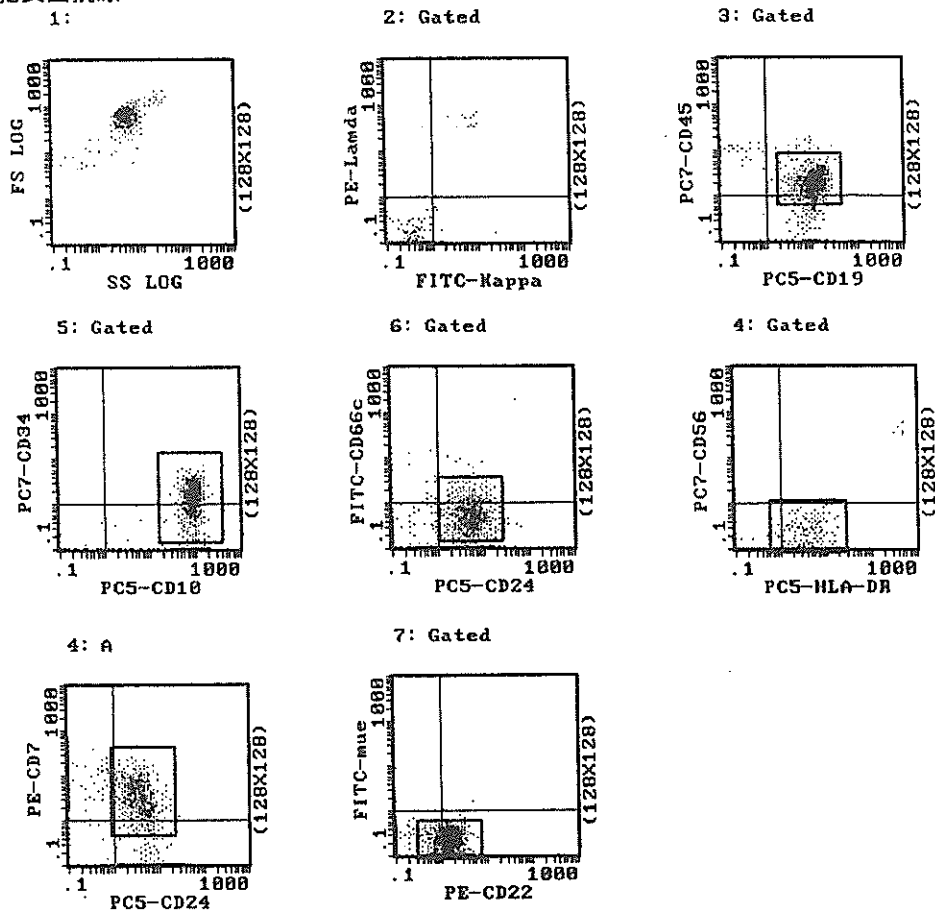
細胞質内抗原

Figure 2 症例1
FS/SS-gatingで診断が容易であった，典型的なB-precursor ALL症例のマーカー結果のヒストグラムを示す。

は，標識する蛍光色素の違いによる反応性の差はほとんどの場合で認められず，標識色素の違いによる陽性/陰性の判定の不一致はなかった。

小児ALLでは，初診時検体中の芽球の割合が高い場合が比較的多いため，MoAbの組み合わせを工夫することによってCD45-gatingを行わなくても，診断に苦慮するケースは少ないと考えられた。実際にこのパネルを用いて行った解析の結果の一例をFigure 2に示す。9割以上の症例では症例1のように，芽球の割合が比較的高く，CD45-gatingを行わなくても，通常のFS/SS-gatingのみで診断可能であった（Figure 2）。しかし，一部の症例では芽球の占める割合が非常に低く，診断
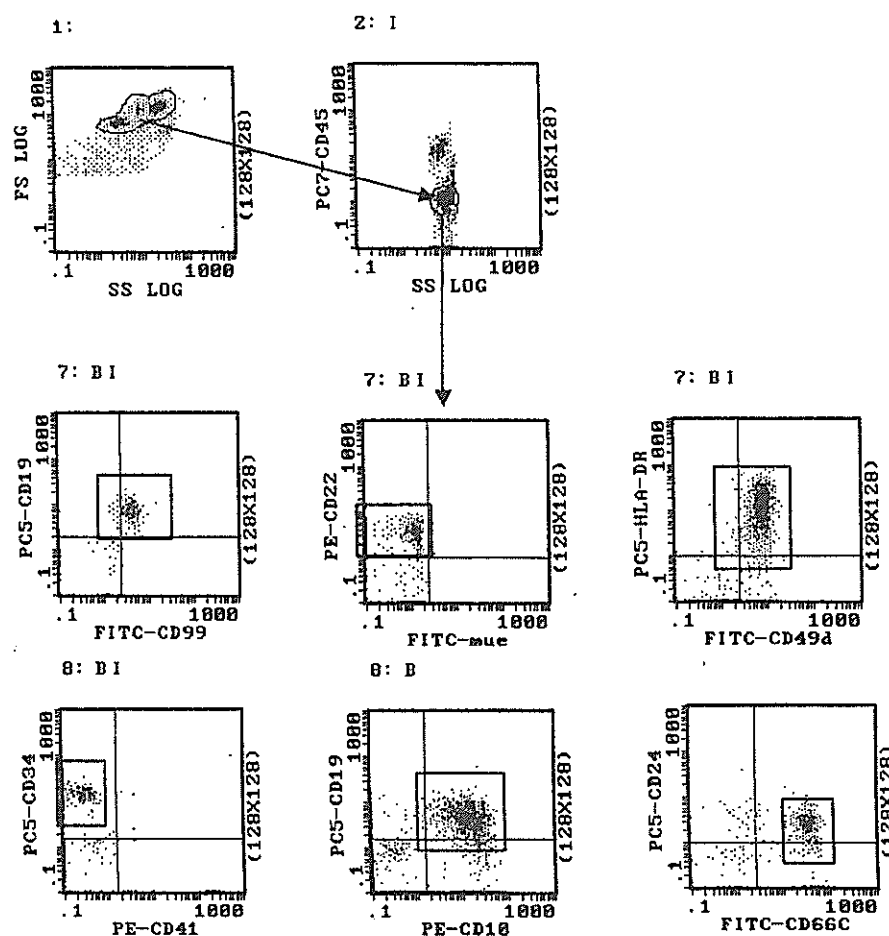
症例2（CD45-gating）

細胞表面抗原

Figure 3　症例2
検体中の芽球の割合が低く，CD45-gatingが診断に有用であった，B-precursor ALL症例のマーカー結果のヒストグラムを示す。

にCD45-gatingが有用な場合も経験された（Figure 3）。

List mode data（LMD）コンペンセーションを用いた解析

　FC500では，一度取得したLMDにコンピューター上でコンペンセーションをかけ直すことが可能である。検体量が少ないために再検査を行うことが困難な場合に非常に有用であった。実際に，データ取得時の蛍光補正が不充分であり，LMDコンペンセーションによって解析し直した例をFigure 4に示す。

考　　察

　近年の化学療法を中心とした集学的治療の進歩により，小児ALL患者の予後は70-80%以上と飛躍的に改善してきた[1]。的確な治療を開始するためには，より正確で迅速な診断が求められるようになっており，FCMによるマーカー検査は，ALLの免疫学的診断において重要な役割を担っている[2]。しかし，一方で約15%の症例が不幸な転帰をたどると言われており[3]，治療成績の一層の向上のためには，治療開始時における的確なリスク分けが必要である。そのためには，従来用いられてきた細胞マーカーや特定の染色体異常の有無などによる病型診断に加えて，治療反応性を評価するためのMRDの検索が重要であるとの報告があいついでいる。また，今後あらたな予後マーカーを捜していく上で，臨床検体を用いたトランスレーショナルリサーチが不可欠であり，そのためには診断に用いた残余細胞を効率的に保存して，より有効に研究に活用して
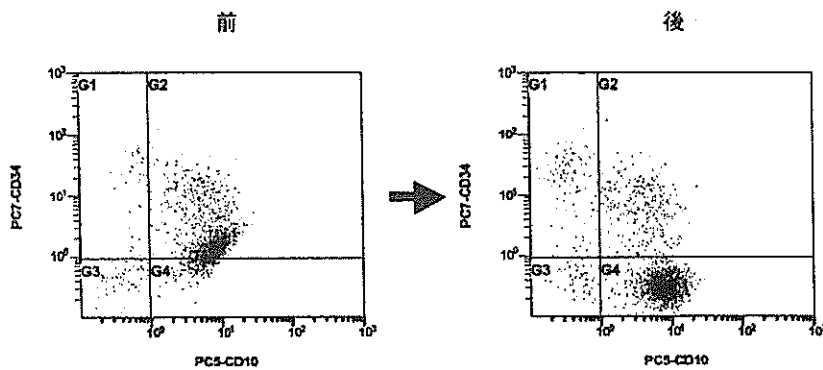
リストモードデータ　コンペンセーション

前　　　　　　　　　　　　　　　　後

Figure 4　リストモードコンペンセーション
一度取得したリストモードデータにコンピューター上でコンペンセーションをかけ直した一例を示す。

行くことが必要である。

　今回われわれが行った検討では，DG-FCMを用いた4カラー解析は，小児ALLの細胞表面マーカー検査において，より少ない細胞数で正確かつ迅速な診断が可能であり，貴重な検体を節約して用いる上で有用であると考えられた。例えば，我々が用いている抗体のパネルでは，細胞質内抗原として必須の検査項目と考えられるCD3，CD79a，TdT，MPOを1本のチューブで測定することが可能である（Table 1）。また，FC500はLMDをワークステーション上で蛍光補正し直すことが可能であり，再検が困難な臨床検体の解析には有用性が高いと考えられた。Luiderら[4]も，FC500を用いた5カラー解析により，白血病の診断パネルにおいて，4カラー解析で17チューブ必要であったものを13チューブに，リンパ腫においては，13チューブから7チューブに減らすことができ，MoAbにかかるコスト（約20%の削減），解析にかかる時間・労力を削減できたと報告している。

　FCMは，白血病などの造血器腫瘍における初期の免疫学的な病型診断とともにMRDの検出においても広く用いられるようになってきている[5-7]。われわれのXLおよびFC500を用いた4カラー解析による検討でも，これまでの報告と同様に−10⁴程度までのMRDを検出することが可能であり（data not shown），今後DG-FCMを用いたマルチカラー解析がMRD検索においても大きな力を発揮することが期待される。

　1チューブについて染色する抗体の項目数を増やすことは，検体量節約のみではなく，複数の抗体で同時に染色することにより各抗原の発現様式を多角的に解析することができる，という利点がある。例えば，抗体の組み合わせを工夫することにより，B-precursor ALL細胞上に発現するCD33，CD65，CD66cといったabberantな抗原の発現をより正確に解析することも可能である。しかし，一回に染色する抗体数を増やすと，蛍光補正がより複雑になることや，抗体同士の競合によってそれぞれの抗体の反応性が修飾されること，等の問題点が生じる。今回われわれが行った4カラー解析では，MoAbの組み合わせを工夫することによって，蛍光補正は比較的容易に行うことができた。また，抗体同士の競合に関する問題も，十分な事前検討を行うことにより，回避することが可能と考えられる。

　一方，小児ALLの場合，その多くの症例ではCD45-gatingは必ずしも必要ではないと考えられる。しかし，一部には芽球の割合が低いために，やはりCD45-gatingが必要な症例が確実に存在することも事実である。検体量を節約しつつ，CD45-gatingが必要な症例にも対応するために，現在5カラー/ CD45-gatingを用いた解析のシステムについて検討を行っている。

　本論文の要旨は，第15回日本サイトメトリー学会（2005年7月，名古屋）で発表した。

参考文献

1) Pui C-H, Evans WE. Treatment of acute lymphoblastic leukemia. N Engl J Med. 2006;354:166-178.

2) Howard SC, Campana D, Coustan-Smith E, et al. Development of a regional flow cytometry center for diagnosis of childhood leukemia in central America.

Leukemia. 2005;19:323-325.

3) Gaynon PS. Childhood acute lymphoblastic leukemia and relapse. Br J Haematol. 2005;131:579-587.

4) Luider J, Cyfra M, Johnson P, Auer I. Impact of the new Beckman coulter cytomics FC500 5-color flow cytometer on a regional flow cytometry clinical laboratory service. Lab Hematol. 2004;10:102-108.

5) Campana D, Coustan-Smith E. Detection of minimal residual disease in acute leukemia by flow cytometry. Cytometry. 1999;38:139-152.

6) Dworzak MN, Froschl G, Printz D, et al. Prognostic significance and modalities of flow cytometric minimal residual disease detection in childhood acute lymphoblastic leukemia. Blood. 2002;99:1952-1958.

7) Borowitz MJ, Pullen DJ, Shuster JJ, et al. Minimal residual disease detection in childhood precursor-B-cell acute lymphoblastic leukemia: relation to other risk factors. A children's oncology group study. Leukemia. 2003;17: 1566-1572.

別冊請求先：〒157-0074　東京都世田谷区大蔵2-10-1
国立成育医療センター研究所　発生・分化研究部　塩沢裕介
TEL: 03-5494-7120, 内線4620　FAX: 03-3416-0181　E-mail: y-shio@mte.biglobe.ne.jp

Involvement of insulin-like growth factor-I and insulin-like growth factor binding proteins in pro–B-cell development

Tomoko Taguchi[a,b], Hisami Takenouchi[a], Jun Matsui[a], Wei-Ran Tang[a], Mitsuko Itagaki[a], Yusuke Shiozawa[a], Kyoko Suzuki[a], Sachi Sakaguchi[a], Yohko U. Ktagiri[a], Takao Takahashi[b], Hajime Okita[a], Junichiro Fujimoto[a], and Nobutaka Kiyokawa[a]

[a]Department of Developmental Biology, National Research Institute for Child Health and Development,
Setagaya-ku, Tokyo; [b]Department of Pediatrics, Keio University, School of Medicine, Shinjuku-ku, Tokyo, Japan

Objective. Insulin-like growth factor (IGF)-binding proteins (IGFBPs) are a family of proteins thought to modulate IGF function. By employing an in vitro culture system of human hematopoietic stem cells cocultured with murine bone marrow stromal cells, we examined the effects of IGF-I and IGFBPs on early B-cell development.

Materials and Methods. Human CD34+ bone marrow cells were cocultured with murine stromal MS-5 cells for 4 weeks, and pro–B-cell number was analyzed by flow cytometry. After administration of reagents that are supposed to modulate IGF-I or IGFBP function to the culture, the effect on pro–B-cell development was examined.

Results. After cultivation for 4 weeks, effective induction of pro–B-cell proliferation was observed. Experiments using several distinct factors, all of which neutralize IGF-I function, revealed that impairment of IGF-I function results in a significant reduction in pro–B-cell development from CD34+ cells. In addition, when the effect of recombinant proteins of IGFBPs and antibodies against IGFBPs were tested, IGFBP-3 was found to inhibit pro–B-cell development, while IGFBP-6 was required for pro–B-cell development.

Conclusions. IGF-I is essential for development of bone marrow CD34+ cells into pro-B cells. Moreover, IGFBPs are likely involved in regulation of pro–B-cell development. © 2006 International Society for Experimental Hematology. Published by Elsevier Inc.

Insulin-like growth factor-I (IGF-I) is an anabolic hormone and, like growth hormone and insulin, regulates whole body growth, metabolism, tissue repair, and cell survival [1]. In addition to its main production by the liver, IGF-I is also produced by bone marrow (BM) stromal cells, myeloid cells, and peripheral lymphocytes. In plasma and most biological fluids, IGF-I binds to members of a family of six specific soluble proteins, known as IGF-binding proteins (IGFBPs) 1–6, all of which have structures that are unrelated to those of IGF receptors (IGFRs) [2]. Although IGFBPs were originally described as passive circulating transport proteins, they are now recognized as playing a variety of roles in circulation, the extracellular environment, and inside the cell [3,4].

Of the six IGFBPs, IGFBP-3 is the most abundant IGFBP in plasma. In vitro experiments examining the effects of IGFBP-3 on various cell cultures have provided conflicting data, with both enhancement and inhibition of IGF-I actions, depending upon the cell type and culture conditions used [3,4]. In contrast, IGFBP-6 was purified from human cerebrospinal fluid and from transformed human fibroblast cell culture [3]. IGFBP-6 has been shown to inhibit IGF actions, including proliferation, differentiation, cell adhesion, and colony formation of osteoblasts and myoblasts [4]. Although the IGFBPs differ in their structure and binding specificity, functional differences among the various IGFBPs are still not clear [4].

In view of its multiple effects, IGF-I is thought to play an integral role in hematopoiesis [1]. IGF-I stimulates growth of bones and seems to control the volume of BM, thereby regulating production of hematopoietic cells [5]. Moreover, IGF-I has been suggested to have direct effects on development of a variety of hematopoietic cells. In the case of

Offprint requests to: Tomoko Taguchi, M.D., Ph.D., Department of Developmental Biology, National Research Institute for Child Health and Development, 2-10-1, Okura, Setagaya-ku, Tokyo 154-8535, Japan; E-mail: ttaguchi@nch.go.jp

B-cell development in mice, for example, previous reports have indicated that IGF-I stimulates maturation of pro-B cells into pre-B cells [6] and acts as a B-cell proliferation cofactor to synergize with the activity of interleukin (IL)-7 [7]. Indeed, administration of IGF-I increased the number of pre-B cells in BM and splenic B cells in normal mice and after BM transplantation [8]. However, the effect of IGF-I on B-cell development, especially in humans, is still largely unknown. In addition, although murine BM stromal cells secrete IGFBPs, the functional role of them in hematopoiesis remains unclear.

In an attempt to clarify the effect of IGF-I and IGFBPs on early B-cell development, we employed an in vitro culture system of human hematopoietic stem cells (HPSCs) cocultured with murine BM stromal cells that induce pro-B cells. In this article, we expand upon results of previous reports by other authors [6–8] and show that IGF-I is essential for pro–B-cell induction from HPSCs. In addition, we also report that IGFBP-3 inhibits pro–B-cell development, whereas IGFBP-6 is required for pro–B-cell development. The possible role of IGFBPs in early B-cell development is discussed.

Materials and methods

Reagents
Recombinant human and mouse IGF-I, IGFBPs, and the IGF-IR kinase inhibitor I-OMe-AG538 were obtained from PeproTech EC Ltd. (London, UK), G-T Research Products (Minneapolis, MN, USA), and Calbiochem-Novabiochem Co. (San Diego, CA, USA), respectively. All reagents are solved in phosphate-buffered saline, except I-Ome-AG538, which is solved in dimethyl sulfoxide, and diluted to the indicated concentration by culture medium.

The following mouse monoclonal antibodies (mAbs) against human antigens were used: anti-IGF-IR from G-T; purified anti-CD19, fluorescein isothiocyanate (FITC)-conjugated anti-μ heavy chain, and phycoerythrin (PE)-conjugated anti-κ and anti-λ light chains and anti-CD25 from Becton Dickinson Biosciences (San Diego, CA, USA); FITC-conjugated anti-CD24, CD43, and CD45, PE-conjugated anti-CD10, CD20, CD33, and CD179a, and PE-cyanine (PC)-5–conjugated anti-CD19 from Beckman/Coulter Inc. (Westbrook, MA, USA). The CD179a molecule, also known as VpreB, is a component of surrogate light chain and is specifically expressed in B-cell precursors, including pro-B and pre-B cells, but not in mature B cells [9]. Hamster mAb against mouse IGF-I and goat polyclonal anti-mouse IGF-I, and IGFBPs Abs were obtained from G-T. Rabbit polyclonal Abs against human IGF-IR and phosphospecific IGF-IR were purchased from Cell Signaling Technology (Beverly, MA, USA). Goat polyclonal anti–β-actin Ab was obtained from Santa Cruz Biotechnology, Inc. (Santa Cruz, CA, USA). Secondary Abs were obtained from Molecular Probes, Inc. (Eugene, OR, USA), and Dako Cytomation, Co. (Glostrup, Denmark), respectively. All other chemical reagents were obtained from Wako Pure Chemical Industries, Ltd. (Osaka, Japan), unless otherwise indicated.

Cells and cultures
Human BM CD34$^+$ cells purchased from Cambrex Bio Science Walkersville, Inc. (Walkersville, MD, USA) were used. These cells had been isolated from human tissue after obtaining informed consent. A cloned murine BM stromal cell line, MS-5, was kindly provided by Dr. A. Manabe (St. Luke's International Hospital, Tokyo, Japan) and Dr. K. J. Mori (Nigata University, Nigata, Japan). Human B-precursor acute lymphoblastic leukemia cell line NALM-16 was kindly provided by Dr. Y. Matsuo (Grand Saule Immuno research Laboratory, Nara, Japan) and was maintained in RPMI-1640 supplemented with 10% (v/v) fetal calf serum (FCS; Sigma-Aldrich Fine Chemical Co., St. Louis, MO, USA) at 37°C in a humidified 5% CO_2 atmosphere.

For induction of pro-B cells, MS-5 cells were plated at a concentration of 1×10^5 cells on a 12-well tissue plate (Asahi Techno Glass Co., Chiba, Japan). The next day, 4×10^4 cells/well/2 mL CD34$^+$ cells were plated onto the MS-5 cells in culture medium supplemented with 10% FCS and various combinations of reagents, as indicated in the figures. Because our preliminary experiments revealed that cultures in an RPMI-1640 medium produced a higher yield of B cells compared with cultures in α-minimum essential medium (data not shown), we used RPMI-1640 medium for the following experiments. After cultivation for the indicated periods, cells were harvested using 0.25% trypsin plus 0.02% ethylenediamine tetraacetic acid (IBL Co. Ltd., Gunma, Japan), and the number of cells per well was determined. All experiments were performed in triplicate, and means ± standard deviations (SD) of cell numbers are shown in Figures 1C, 3, 4, 5C, and 5D. For the histology studies, cells were cultured on type-I collagen-coated cover slips (Asahi Techno Glass) and were examined by May-Grünwald-Giemsa staining or immunohistochemical staining.

Immunofluorescence study
A multicolor immunofluorescence study was performed using a combination of FITC, PE, and PC-5. Cells were stained with fluorescence-labeled mAbs and analyzed by flow cytometry (EPICS-XL, Beckman/Coulter), as described previously [10]. Staining of the cytoplasmic antigens was performed using Cytofix/Cytoperm Kits (Becton Dickinson), according to manufacturer's protocol. To detect surface immunoglobulin (Ig)$^+$ mature B cells and cytoplasmic μ$^+$ pre-B cells simultaneously, cells were first stained with a mixture of PC-5-conjugated anti-CD19 Ab and PE-conjugated Abs against κ/λ light chains and then treated with cell permeabilization reagents followed by staining of cytoplasmic antigens. It was confirmed by preliminary experiments that permeabilization treatment does not affect the signals of surface antigens stained beforehand. For cell sorting, human BM CD34$^+$ cells cocultured with MS-5 for 4 weeks were harvested and stained with PC-5-conjugated anti-CD19 mAb. CD19$^+$ cells were sorted in an EPICS-ALTRA cell sorter (Beckman/Coulter). For CD19 immunostaining, cover slips were fixed with ice-cold acetone for 15 minutes and stained with anti-CD19 mAb and examined by confocal laser scanning microscope (FV500; Olympus, Tokyo, Japan) as described previously [11].

RT-PCR, immunoblotting, and detection of IGF-I
Total RNA was extracted from cultured cells, and reverse transcriptase polymerase chain reaction (RT-PCR) was performed as described previously [12]. The sets of primers used in this study are listed in Table 1. Cell lysates were prepared by solubilizing the cells in lysis buffer and immunoblotting was performed as described previously [13]. The concentration of mouse IGF-I in
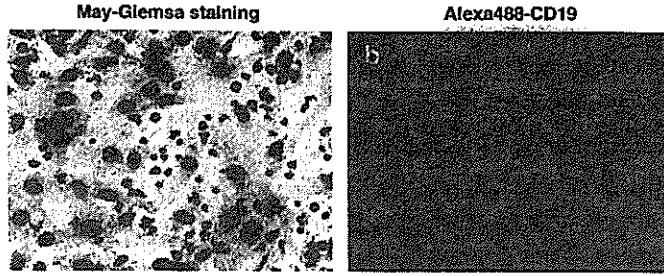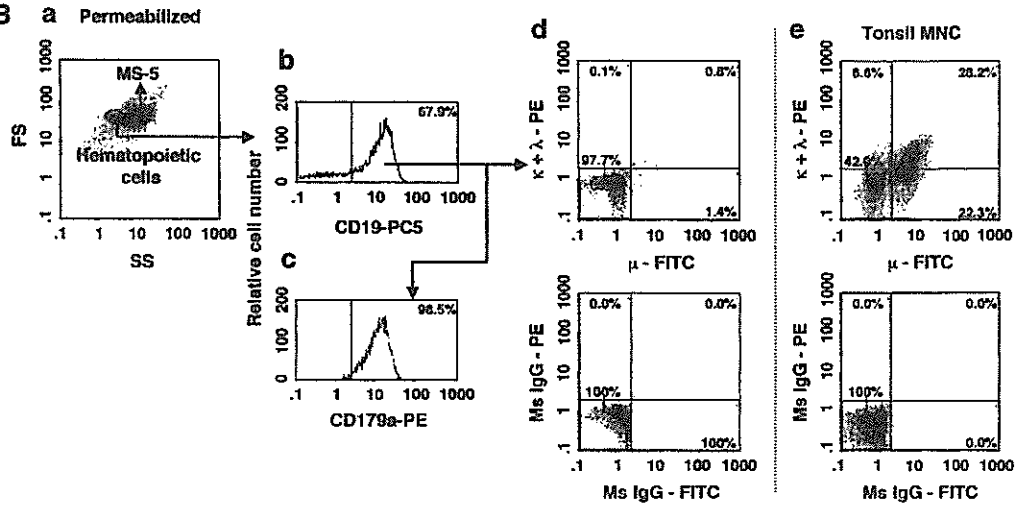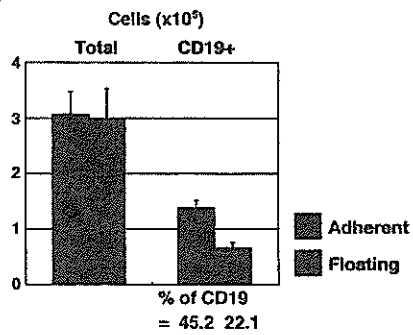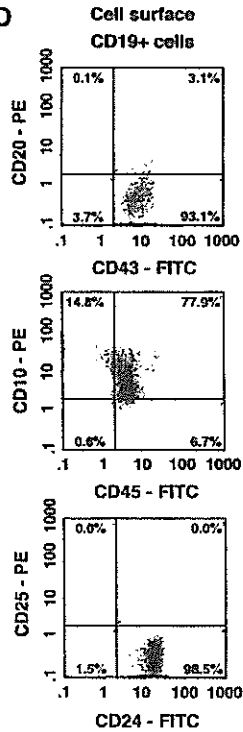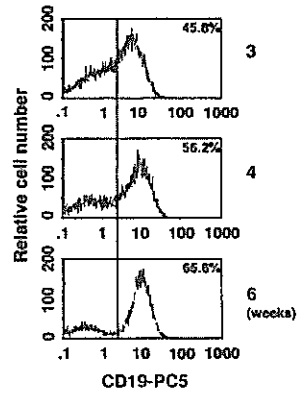
culture supernatants of MS-5 cells was determined by sandwich enzyme-linked immunosorbent assay (ELISA), using Mouse IGF-I Quantikine ELISA Kit (R&D Systems, Wiesbaden, Germany), according to manufacturer's instruction. Experiments were performed in triplicate, and mean ± SDs of cell numbers are shown in Figure 2C.

Results

Differentiation of
pro-B cells from human BM CD34$^+$ cells by
coculturing with murine stromal MS-5 cells
Murine stromal cell line MS-5 has been reported to possess the capability to support differentiation of B-lineage cells from human cord blood (CB) CD34$^+$ cells [14–17]. Coincident with these previous reports, we observed that human BM CD34$^+$ cells generated a high number of CD19$^+$ B cells after cocultivation with MS-5 cells (Fig. 1A and B). Starting with 4×10^4 CD34$^+$ cells, approximately 0.4 to 1.3×10^6 mononuclear cells, 30.1% to 68.2% of which were CD19$^+$ cells, were obtained after 4 weeks of cultivation. As shown in Figure 1C, approximately half of the hematopoietic cells were floating, while the remainder were adhered to the MS-5 cells and the CD19$^+$ cells were more abundant in adherent cell fraction.

As shown in Figure 1B, most of the CD19$^+$ B cells obtained after 9 weeks of cultivation expressed cytoplasmic CD179a. The CD179a is reported to be already expressed in pro-B cells, remains expressed on B-cell precursors, and disappears upon differentiation from pre-B cells to mature B cells [9]. In contrast, a few percent of CD19$^+$ cells were positive for surface and/or cytoplasmic μ heavy chain and a portion of them expressed either the κ or λ light chains (Fig. 1B). We also observed that CD10, CD24, CD43, and CD45 were expressed but CD20 and CD25 were not in the CD19$^+$ cells (Fig. 1D). No difference in immunophenotypic characteristics was observed between the CD19$^+$ cells in adherent cell fraction and that in floating cell fraction (data not shown). Based on the above data, we concluded that human BM CD34$^+$ cells can differentiate into pro-B cells, but not into pre-B cells, after cocultur-

ing with the murine stromal cell line MS-5 in the present culture system. CD19$^+$ cells cultured for 4 weeks were also examined, and similar immunophenotypic characteristics were noted (data not shown).

Next, we examined the time course of the expression of CD19 in human BM CD34$^+$ cells in our culture system. CD19$^+$ cells were already detected after 1 week of culture (data not shown), and the number of CD19$^+$ cells increased throughout the course of the cell culture thereafter. After 4 to 9 weeks of culture, both the fluorescent intensity of CD19 on each cell and the percentage of CD19$^+$ cells out of the total number of cells continued to increase (Fig. 1E), but the total number of CD19$^+$ cells did not change significantly (data not shown). When expression of transcription factors related to early B-cell differentiation was analyzed by RT-PCR, expression profiles of these factors were well correlated with proliferation of CD19$^+$ cells as described (data not shown). Therefore, pro–B-cell development after 4 weeks of culture in the present system was analyzed in the following experiments.

Effect of IGF-I on
in vitro human pro–B-cell development
Because expression of IGFRs in cultured CD34$^+$ BM cells was detected (Fig. 2A), we first tested the effect of adding exogenous recombinant human IGF-I to the coculture of CD34$^+$ BM cells and MS-5 cells to evaluate the contribution of IGF-I to human pro–B-cell development; no significant change in pro–B-cell development was observed (data not shown).

However, RT-PCR analysis revealed expression of IGF-I in MS-5 cells (Fig. 2B). Results of ELISA further demonstrated that mouse IGF-I was indeed secreted in the culture supernatant of MS-5 cells (Fig. 2C). As presented in Figure 2D, mouse IGF-I is active in human hematopoietic cells and can induce tyrosine-phosphorylation of human IGF-IR expressed on NALM-16 cells derived from human B-precursor acute lymphoblastic leukemia. When we tested similarly, MS-5 culture supernatant could stimulate IGF-IR on NALM-16 cells, whereas freshly prepared medium containing 10% FCS could not, indicating that mouse IGF-I secreted from MS-5 cells is sufficient to stimulate

Figure 1. Characterization of human bone marrow (BM) CD34$^+$ cells cocultured with murine stromal cells. (A) Human BM CD34$^+$ cells were cocultured for 4 weeks with murine stromal MS-5 cells on cover slips. At the end of the culture period, the cells were examined with either May-Grünwald-Giemsa staining (a) or CD19 immunostaining (green) with nuclear counter staining by 4′,6-diamidino-2-phenylindole (blue) (b). Original magnification ×400. (B) Human BM CD34$^+$ cells cocultured for 9 weeks with MS-5 cells were harvested. The expression of cell surface CD19, κ/λ light chains and cytoplasmic CD179a and μ heavy chain was simultaneously assessed by flow cytometry with cell-permeabilization technique as described in Materials and Methods. In cultured BM cells (a), CD19$^+$ cells were gated (b), and expression of CD179a (c), μ heavy chain, and κ/λ light chains (d) was examined. As a negative control, same sample specimen stained with isotype-matched control mouse IgG was also presented. As a positive control, mononuclear cells prepared from tonsil were similarly treated as in (d) and presented (e). FITC = fluorescein isothiocyanate; FS = forward light scatter; SS = side light scatter. (C) Human BM CD34$^+$ cells were cocultured with MS-5 cells for 4 weeks and the adherent cell fraction and floating cell fraction were collected separately. Total cell number and expression of CD19 were examined as above. (D) Human BM CD34$^+$ cells were cocultured with MS-5 cells as in (B), and multicolor immunofluorescence study was performed as above. CD19$^+$ cells were gated, and expression of surface B-cell differentiation markers, as indicated, was examined using flow cytometry. (E) Human BM CD34$^+$ cells were cocultured with MS-5 cells for 3, 4, and 6 weeks, and expression of CD19 was examined using flow cytometry.